

# **THE DEVELOPMENT OF AN INNOVATIVE THERMAL MIXING TECHNIQUE FOR THE FABRICATION OF LARGE SCALE POLYMETHACRYLATE MONOLITHS**

**CHAN YI WEI**



**THESIS SUBMITTED IN FULFILLMENT FOR  
THE DEGREE OF MASTER OF SCIENCE**

**BIOTECHNOLOGY RESEARCH INSTITUTE  
UNIVERSITI MALAYSIA SABAH  
2017**

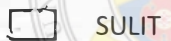
**UNIVERSITI MALAYSIA SABAH**  
**BORANG PENGESAHAN STATUS TESIS**

JUDUL: **THE DEVELOPMENT OF AN INNOVATIVE THERMAL MIXING  
TECHNIQUE FOR THE FABRICATION OF LARGE SCALE  
POLYMETHACRYLATE MONOLITHS**

IJAZAH: **SARJANA SAINS (BIOTEKNOLOGI)**

Saya **CHAN YI WEI**, Sesi **2013-2017**, mengaku membenarkan tesis Sarjana ini disimpan di Perpustakaan Universiti Malaysia Sabah dengan syarat-syarat kegunaan seperti berikut:-

1. Tesis ini adalah hak milik Universiti Malaysia Sabah
2. Perpustakaan Universiti Malaysia Sabah dibenarkan membuat salinan untuk tujuan pengajian sahaja.
3. Perpustakaan dibenarkan membuat salinan tesis ini sebagai bahan pertukaran antara institusi pengajian tinggi.
4. Sila tandakan (/):



SULIT

(Mengandungi maklumat yang berdarjah keselamatan atau kepentingan Malaysia seperti yang termaktub di dalam AKTA RAHSIA 1972)



TERHAD

(Mengandungi maklumat TERHAD yang telah ditentukan oleh organisasi/badan di mana penyelidikan dijalankan)



TIDAK TERHAD

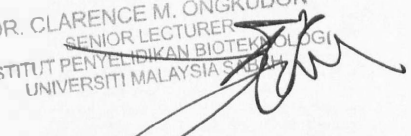


**CHAN YI WEI**  
**MZ1321003T**

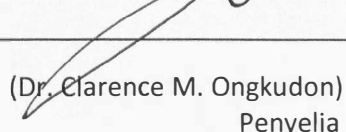
Disahkan Oleh,

  
**NURULAIN BINTI ISMAIL**  
LIBRARIAN  
UNIVERSITI MALAYSIA SABAH

(Tandatangan Pustakawan)

  
**DR. CLARENCE M. ONGKUDON**  
SENIOR LECTURER  
INSTITUT PENYELIDIKAN BIOTEKNOLOGI  
UNIVERSITI MALAYSIA SABAH

Tarikh : 07 SEPTEMBER 2017

  
(Dr. Clarence M. Ongkudon)  
Penyelia

## **DECLARATION**

I hereby declare that the content of this thesis is my own except for quotations, equations, summaries and references, which have been duly acknowledged. The developed technology is currently pending for patent approval, thus the thesis should be kept confidential and not made publicly available without the prior consent of the inventor and UMS.

30<sup>th</sup> August 2017



**UMS**  
UNIVERSITI MALAYSIA SABAH  
  
Chan Yi Wei  
MZ1321003T

# CERTIFICATION

NAME : **CHAN YI WEI**  
MATRIC NO. : **MZ1321003T**  
TITLE : **THE DEVELOPMENT OF AN INNOVATIVE  
THERMAL MIXING TECHNIQUE FOR THE  
FABRICATION OF LARGE SCALE  
POLYMETHACRYLATE MONOLITHS**  
DEGREE : **MASTER OF SCIENCE (BIOTECHNOLOGY)**  
DATE OF VIVA : **18 JULY 2017**

1.

**SUPERVISOR**

Dr. Clarence M. Ongkudon



**CERTIFIED BY;**

**UMS**

Signature

A handwritten signature in black ink, appearing to read "DR. CLARENCE M. ONGKUDON".

DR. CLARENCE M. ONGKUDON  
SENIOR LECTURER  
INSTITUT PENYELIDIKAN BIOTEKNOLOGI  
UNIVERSITI MALAYSIA SABAH

## **ACKNOWLEDGEMENT**

I would like to take this privilege to thank my family for their continuous support throughout my entire master's degree project. My gratitude goes to Dr. Clarence M. Ongkudon, my research supervisor, for his guidance, comments and motivation that helped me to be more independent, think out of the box, creative and innovative during my postgraduate study. Also, not forgetting the lab assistants especially Marlenny Jumadi, Mony Mian and Vidarita Maikin for assisting me in the daily laboratory operation whenever I needed them the most. I would also like to extend my sincere appreciation to my fellow postgraduate friends, Aldrin Felix, Eugene Marfo Obeng, and others for making my research experience in Biotechnology Research Institute of University Malaysia Sabah a memorable one.

Chan Yi Wei

30<sup>th</sup> August 2017



**UMS**  
UNIVERSITI MALAYSIA SABAH

## ABSTRACT

The upsurge of monolith technology has redefined the limit of bioseparation sciences that was previously established by packed-bed column. Polymethacrylate monolith features large pores that are interlinked and give form to continuous pore channels which enable mass transport to transpire under convection manner. To date, there have been many successful attempts in the application of monolith for biomolecules separation using small-scale monoliths. However, the production and application of large-scale monoliths have not received much attention due to challenges pertaining to thermal escalation and wall channeling. The objective of this project is to investigate and elucidate the hurdles in monolith up-scaling and come out with possible solutions to overturn the persisting challenges. In regards to this, polymethacrylate monolith was fabricated through thermal-initiated free radical polymerization for subsequent analysis. A novel strategy involving the use of SEM on partitioned monolith coupled with temperature profiling and pore size distribution modality curves was used to determine the effect of porogen content (%) and thermal expansion on the pore morphology of varied scales of monoliths. Moreover, the effect of mold internal dimension on the magnitude of heat build-up was investigated by fabricating 70 % porogen-containing monoliths in columns that comes with various dimensions. The results showed that pore morphology differs with different monomer concentrations while the intensity of thermal build-up is inversely proportional to the porogen content (%). Also, the homogeneity of monoliths was observed to be directly proportional to porogen content (%) and inversely proportional to thermal build-up. The column internal diameter (i.d) analysis revealed that thermal escalation ceased beyond 8 cm i.d monolith while the changes of pore morphology and uniformity remained unchanged from 5 cm i.d onwards. However, the increased column diameter resulted in poorer heat transfer and was clearly illustrated by the large peak width of 17.0 cm i.d. The effect of thermal build-up on pore morphology and homogeneity was attributed to fixated differences in porogen content (%). In conclusion, the significant disparity of pore size distribution profile of various sections was not observed albeit improvement was recognized with reduced heat accumulation. Based on the preliminary studies conducted, thermal minimization method was devised as the countermeasure to reduce the heat escalation. The effectiveness of thermal mixing strategy was validated by successful fabrication of an intact monolith under 70 % porogen content, 5 cm i.d and 150 ml with negligible heat build-up. To improve on its applicable column size range, monolith reactor was designed and built which involved channeling water intermittently in between hot and cold water in accordance with the temperature of core region. In addition, three loop controllers were designed and put into test via fabrication of 17.0 cm i.d, 3.9 L monolith by using the reactor. The results have revealed the 3<sup>rd</sup> loop variant as the most optimal controller by managing to fabricate an intact 17.0 cm i.d monolith up to 3.9 L whereby the highest  $T_{max}$  recorded was 74.63 °C as compared to 124.95 °C and 122.28 °C achieved by the other two controllers respectively. The success of this method will pave the way for the future through which mass production of therapeutic drugs with monolith of liter scale is practically feasible.

## **ABSTRAK**

### **PEMBANGUNAN TEKNIK CAMPURAN HABA INOVATIF UNTUK PENGHASILAN MONOLIT POLIMETAKRILAT BERSKALA BESAR**

Kewujudan teknologi monolit telah mengubah definisi had sains bio-pemisahan yang dahulunya hanya didominasi oleh kolumn penapis termampat. Monolit polimetakrilat mempunyai struktur liang besar yang saling bersambung dan ini mewujudkan saluran liang berterusan yang membolehkan pengangkutan jisim berlaku melalui proses perolakan. Sehingga kini, terdapat banyak kejayaan dalam penggunaan monolit skala kecil untuk pemisahan biomolekul. Walau bagaimanapun, penghasilan dan penggunaan monolit berskala besar tidak mendapat banyak perhatian disebabkan beberapa cabaran terutama sekali yang berkaitan dengan peningkatan haba dan saluran dinding. Objektif projek ini adalah untuk mengkaji dan menjelaskan cabaran-cabaran yang dihadapi dalam penghasilan monolit berskala besar sekaligus mencari kaedah-kaedah penyelesaian. Dalam hal ini, monolit polimetakrilat telah dihasilkan melalui pempolimeran radikal bebas yang diaktifkan oleh haba untuk analisis seterusnya. Strategi novel yang melibatkan penggunaan SEM pada monolith yang telah dibahagikan, pemprofilan suhu, dan lengkungan modaliti taburan saiz liang telah digunakan untuk menentukan kesan kandungan porogen (%) dan pengembangan haba pada morfologi liang monolit berbeza skala. Selain itu, kesan dimensi acuan pada magnitud penghasilan haba telah dikaji dengan menggunakan monolit yang mengandungi 70 % porogen dalam kolumn yang berlainan dimensi. Hasil kajian menunjukkan bahawa morfologi liang yang terhasil berbeza pada kepekatan monomer yang berlainan, manakala intensiti pembentukan haba adalah berkadar songsang dengan kandungan porogen (%). Selain itu, keseragaman monolit didapati berkadar langsung dengan kandungan porogen (%) dan berkadar songsang dengan pembentukan haba. Analisis diameter dalaman kolumn (i.d) mendedahkan penemuan baru dimana peningkatan haba berhenti pada 8 cm i.d monolit manakala perubahan morfologi dan keseragaman liang kekal tidak berubah dari 5 cm i.d dan seterusnya. Walau bagaimanapun, penambahan diameter dalaman kolumn menyebabkan masalah pemindahan haba secara berkesan dan jelas digambarkan pada kolumn berkelebaran maksima, 17.0 cm i.d. Kesan peningkatan haba kepada morfologi dan kehomogenan liang adalah disebabkan oleh perbezaan kandungan porogen (%). Kesimpulannya, tidak ada perbezaan yang ketara dalam analisis profil taburan saiz liang di antara semua bahagian monolit tetapi ianya bertambah baik dengan pengurangan haba terkumpul. Berdasarkan kajian awal yang dijalankan, kaedah pengurangan haba telah dipilih sebagai langkah untuk mengurangkan peningkatan haba. Keberkesanan teknik campuran pemanasan dan penyejukan berjaya dibuktikan apabila monolit tanpa rekahan yang mempunyai diameter 5 cm dan isipadu 150 ml berjaya dihasilkan dengan kesan pembentukan haba berlebihan minima. Untuk meningkatkan saiz monolit yang boleh dihasilkan menggunakan cara ini, reaktor monolit telah direka dan dibina dimana ianya melibatkan pengaliran air panas dan sejuk setara dengan suhu pusat monolit. Di samping itu, tiga jenis sistem kawalan telah direka dan diuji melalui fabrikasi monolit 17.0 cm i.d, 3.9 L dengan menggunakan reaktor tersebut. Keputusan ujikaji telah mendedahkan bahawa sistem kawalan jenis ketiga sebagai kaedah paling

*optimum dengan kejayaan yang dicapai melalui penghasilan monolit tanpa rekahan yang mempunyai diameter 17.0 cm dan isipadu 3.9 L. Sistem ini juga berjaya mengurangkan pembentukan haba kepada suhu 74.63 °C berbanding 124.95 °C dan 122.28 °C yang dicapai oleh dua sistem kawalan lain. Keberkesanan kaedah ini akan membolehkan pengeluaran besar-besaran ubat terapeutik dengan monolit berskala liter di masa depan lebih praktikal.*



**UMS**  
UNIVERSITI MALAYSIA SABAH

# TABLE OF CONTENTS

	Page
<b>TITLE</b>	i
<b>DECLARATION</b>	ii
<b>CERTIFICATION</b>	iii
<b>ACKNOWLEDGEMENT</b>	iv
<b>ABSTRACT</b>	v
<b>ABSTRAK</b>	vi
<b>TABLE OF CONTENTS</b>	viii
<b>LIST OF TABLES</b>	xii
<b>LIST OF FIGURES</b>	xiii
<b>LIST OF ABBREVIATIONS</b>	xx
<b>CHAPTER 1: INTRODUCTION</b>	1
1.1    Background of Study	1
1.2    Problem Statement	4
1.3    Hypothesis of Study	5
1.4    Objectives	5
1.5    Significance of Research	5
<b>CHAPTER 2: LITERATURE REVIEW</b>	6
2.0    Introduction	6
2.1    Advantages of Using Monolith in Industrial Application	6
2.1.1    Lower Dispersion in Chromatographic Purification	6
2.1.2    Rapid Processing of Biomolecules	7
2.1.3    High Binding Capacity for Biomolecule Processing	7
2.1.4    Wide Range of Biomolecular Purification	7
2.1.5    Less Susceptible to Clogging	8
2.2    Types of Monolith Feedstock	8

2.2.1	Agarose Monolith	8
2.2.2	Silica Monolith	9
2.2.3	Cryogels	10
2.2.4	Polymethacrylate Monolith	11
2.3	Mechanism of Monolith Fabrication	13
2.4	Barriers in Fabrication of Large Volume Monolith	13
2.5	Existing Countermeasure in Fabrication of Preparative Scale Monolith	14
2.5.1	Thermal-Based Strategies	15
2.5.1.1	Frontal Polymerization	15
2.5.1.2	Supercritical CO <sub>2</sub> as Porogen	16
2.5.1.3	Gradual Addition of Monomer Mixtures	17
2.5.1.4	Metathesis Polymerization	17
2.5.1.5	Variant Source of Irradiation	18
2.5.1.6	Cooling-Mediated Polymerization	18
2.5.2	Template-Based Porosity	20
2.5.2.1	Agarose Gel Template	20
2.5.2.2	PMMA Template	21
2.5.2.3	PFA-F127 Template	21
2.5.2.4	Polypropylene Oxide Template	21
2.5.2.5	Porous Silica Bead Template	22
2.5.2.6	High Internal Phase Emulsion Template	22
2.5.2.7	Altered Freeze-Casting Monolith	23
2.5.2.8	Polymer Shielded – Nanocapsule Building Block	24
2.5.3	Wall Channels Elimination	26
2.5.3.1	Induction of Swelling	26
2.5.3.2	Covalent Attachment to Column	26
2.5.3.3	Non-Shrinking Monolith Adsorbent	26
2.5.3.4	Conical Column	27
2.6	Future Prospective of Preparative Scale Monolith Development	27

<b>CHAPTER 3: MATERIALS AND METHODOLOGY</b>	29
3.0 Introduction	29
3.1 Materials and Chemicals	29
3.2 Synthesis of Poly (GMA-EDMA) Monolithic Column	29
3.3 Temperature Profile Analysis	30
3.4 SEM Analysis	30
3.5 Pore Size Distribution Analysis	31
3.6 Monolith Porosity Analysis	31
3.7 Thermal Mixing - Exothermic Heat Minimization Strategy	32
3.8 Pump-driven Monolith Reactor (MR-03)	33
3.8.1 Development of Controller	33
3.8.1.1 1 <sup>st</sup> Run/Response Loop	33
3.8.1.2 2 <sup>nd</sup> Run/Response Loop – 10 Minutes Gap to T <sub>sp</sub>	34
3.8.1.3 3 <sup>rd</sup> Run/Response Loop – Maintaining the Core	34
Temperature at 45°C	
3.9 Thermal Imaging Analysis	34
<b>CHAPTER 4: RESULTS AND DISCUSSION</b>	37
4.1 Determination of Monolith's Homogeneity	37
4.1.1 Limitation of Mean Pore Size Analysis	39
4.1.2 Mean Pore Size vs Pore Size Distribution Analysis	39
4.2 The Effect of Varied Porogen Content on Large Scale Polymethacrylate Monolith	42
4.2.1 Thermal Expansion Analysis	42
4.2.2 Pore Size Distribution Analysis	46
4.2.3 SEM Analysis	51
4.3 Effect of Mold's Internal Diameter (i.d) on Magnitude of Thermal Build-up and Pore Morphology	55
4.3.1 Maximum Exotherm	55
4.3.2 Plateau Effect of Thermal Build-up on Pore Morphology	56
4.4 Limiting Factor of Effect of Thermal Build-up on Pore Morphology	60
4.4.1 Porogen Content as the Limiting Factor	60

4.4.2	Monolith Homogeneity – From Macroscopic Perspective	64
4.5	Thermal Mixing Strategy	66
4.5.1	Effectiveness of Thermal Mixing Method	66
4.6	Monolith Reactor – Design and Build	71
4.6.1	Monolith Reactor (MR-03)	71
4.6.2	Pump-Driven Hydro-Flow	74
4.6.3	Piping configuration of MR-03	77
4.7	Controller-Mediated Fabrication of Monolith	79
4.7.1	Programming of Feedback Controller (Excel Format)	79
4.7.2	Comparison of Three Distinct Loop Variants	81
4.7.3	Thermal Imaging Analysis	84

<b>CHAPTER 5: CONCLUSION</b>	87
------------------------------	----

## REFERENCES

89



## LIST OF TABLES

	Page
Table 2.1: Lists of large volume monolithic columns.	15
Table 4.1: Maximum temperature build-up (°C) recorded at different sections of the monolith and porogen contents (%). Monolith dimension: 150 mL, 5.0 cm column i.d; $T_{poly}$ : 60 °C.	43
Table 4.2: Distinct Modes of Control Loops Variant Configuration.	81



## LIST OF FIGURES

	Page
Figure 2.1: Overall sol-gel process for silica monolith fabrication.	10
Figure 2.2: Overall process employed in cryogels monolith fabrication.	11
Figure 2.3: Schematic representation of the overall fabrication process of agarose gels templated silica monolith. The brown area indicates void space, the white area indicates agarose fibers, the grey area indicates silica gels and the black area indicate pores post agarose gel removal.	20
Figure 2.4: Schematic illustration of the overall synthesis of a porous organic-based monolith using porous silica beads as the pore template.	22
Figure 2.5: SEM image of PolyHIPE monolith featuring bimodal pore size. Pore size (50 – 150 $\mu\text{m}$ )	23
Figure 2.6: Schematic display of modified freeze-casting technique in monolith construction.	24
Figure 2.7: Schematic diagram of the synthesis of nanocapsule featuring cross-linked polymer shell hollow void internal fraction. Amphi-RAFT agent form microemulsion droplets, followed by cross-linking polymerization at the interface of aqueous and surface region of nanocapsule. The paraffin core material is extracted through immersion with tetrahydrofuran and subjected to drying to form hollow fraction of the nanocapsule.	25

Figure 2.8:	Illustration of innovative monolithic column preparation.	27
Figure 3.1:	Comprehensive qualitative SEM analysis on 9 vertical and horizontal sections of the monolith.	30
Figure 3.2:	Intermittent transfer of monolith column in between waterbath and chiller in response to feedback from thermocouple during polymerization process.	32
Figure 3.3:	Schematic diagram of the overall heating mechanism of the pump driven monolith reactor.	35
Figure 3.4:	Schematic diagram of the overall cooling mechanism of the pump driven monolith reactor.	36
Figure 4.1:	SEM images of 70 % monolith at middle outer section featuring macropores and micropores. Monolith dimension: 150 mL monolith; 5.0 cm i.d. Polymerizations were carried out at a constant monomer ratio (EDMA/GMA) of 30/70; porogen concentration of 70 %; polymerization temperature of 60 °C; AIBN concentration of 1 % (w/w) of monomers.	37
Figure 4.2:	Mean pore size analysis across the top section of monolith. Monolith dimension: 150 mL; 5.0 cm i.d. Polymerizations were carried out at a constant monomer ratio (EDMA/GMA) of 30/70; porogen concentrations of 70 %; polymerization temperature of 60 °C; AIBN concentration of 1 % (w/w) of monomers.	39
Figure 4.3:	Pore size distribution analysis throughout the top section of monolith. Monolith dimension: 150 mL; 5.0 cm i.d. Polymerizations were carried out at a constant monomer ratio (EDMA/GMA) of 30/70; porogen concentrations of 70 %.	40

%; polymerization temperature of 60 °C; AIBN concentration of 1 % (w/w) of monomers.

Figure 4.4: Temperature profiling analysis across the top section of monolith. Monolith dimension: 150 mL; 5.0 cm i.d. Polymerizations were carried out at a constant monomer ratio (EDMA/GMA) of 30/70; porogen concentrations of 70 %; polymerization temperature of 60 °C; AIBN concentration of 1 % (w/w) of monomers. 40

Figure 4.5: SEM analysis throughout the top section of monolith. Monolith dimension: 150 mL; 5.0 cm i.d. Polymerizations were carried out at a constant monomer ratio (EDMA/GMA) of 30/70; porogen concentrations of 70 %; polymerization temperature of 60 °C; AIBN concentration of 1 % (w/w) of monomers. 41

Figure 4.6: Temperature build-up profile at varied porogen contents Monolith dimension: 150 mL, 5.0 cm i.d. Polymerizations were carried out at a constant monomer ratio (EDMA/GMA) of 30/70; porogen concentrations of 50 %, 60 % and 70 %; polymerization temperature of 60 °C; AIBN concentration of 1 % (w/w) of monomers. 44

Figure 4.7: a)  $T_{\max}$  of varied porogen content (%) monoliths. b) The duration required to trigger free radical polymerization reaction at each porogen content (%). Monolith dimension: 150 mL, 5.0 cm i.d. Polymerizations were carried out at a constant monomer ratio (EDMA/GMA) of 30/70; porogen concentrations of 50 %, 60 % and 70 %; polymerization temperature of 60 °C; AIBN concentration of 1 % (w/w) of monomers. 45

Figure 4.8:	Cross-comparison of pore size distribution of monoliths containing varied porogen contents at middle inner section. Monolith dimension: 150 mL, 5.0 cm i.d. Polymerizations were carried out at a constant monomer ratio (EDMA/GMA) of 30/70; porogen concentrations of 50 %, 60 % and 70 %; polymerization temperature of 60 °C; AIBN concentration of 1 % (w/w) of monomers.	46
Figure 4.9:	Intra-comparison of effects of a) 50, b) 60 and c) 70 % porogen content on pore size distribution pattern across the axial and radial direction of the monolithic adsorbents. Monoliths dimension: 150 mL, 5.0 cm i.d. Polymerizations were carried out at a constant monomer ratio (EDMA/GMA) of 30/70; porogen concentration of 50 %, 60 % and 70 %; polymerization temperature of 60 °C; AIBN concentration of 1 % (w/w) of monomers.	50
Figure 4.10:	Effects of a) 50 %, b) 60 % and c) 70 % porogen content on surface morphology of polymethacrylate monoliths. Monolith dimension: 150 ml, 5.0 cm i.d. Polymerizations were carried out at a constant monomer ratio (EDMA/GMA) of 30/70; porogen concentration of 50 %, 60 % and 70 %; polymerization temperature of 60 °C; AIBN concentration of 1 % (w/w) of monomers.	54
Figure 4.11:	Effects of mold dimensions on temperature build-up. Polymerizations were carried out at a constant monomer ratio (EDMA/GMA) of 30/70; porogen concentrations 70 %; polymerization temperature of 60 °C; monolith dimensions: 1.5 cm, 5.0 cm, 8.0 cm and 17.0 cm i.d, diameter : height ratio of 1 : 1; AIBN concentration of 1% (w/w) of monomers.	56

- Figure 4.12: Effects of mold dimension on pore size distribution pattern of each partitioned section of the monolithic adsorbent. Polymerizations were carried out at a constant monomer ratio (EDMA/GMA) of 30/70; porogen concentration of 70 %; polymerization temperature 60°C; Monolith Dimension: 1.5 cm, 5.0 cm, 8.0 cm and 17.0 cm i.d, at diameter : height ratio of 1 : 1; AIBN concentration of 1 % (w/w) of monomers. 58
- Figure 4.13: Effects of mold dimension (1.5 cm, 5.0 cm, 8.0 cm and 17.0 cm) on surface morphology of polymethacrylate monoliths. Polymerizations were carried out at a constant monomer ratio (EDMA/GMA) of 30/70; porogen concentrations of 70 %; polymerization temperature of 60 °C; monolith dimensions: 1.5 cm, 5.0 cm, 8.0 cm and 17.0 cm i.d, volume at diameter : height ratio of 1 : 1; AIBN concentration of 1 % (w/w) of monomers. 59
- Figure 4.14: Effects of 60 % vs 70 % porogen contents on maximum temperature gradient and its corresponding effects on pore morphology. Polymerizations were carried out at a constant monomer ratio (EDMA/GMA) of 30/70; porogen concentrations of 60 % and 70 %; polymerization temperature of 60 °C; Monolith Dimension: 5.0 cm, 8.0 cm and 17.0 cm i.d, diameter : height ratio of 1 : 1; AIBN concentration of 1 % (w/w) of monomers. 63
- Figure 4.15: Presence of megapores on both 60 % and 70 % (porogen content) monolithic adsorbents. 64
- Figure 4.16: Porosity analyses of a) 60 % and b) 70 % monoliths fabricated in 17.0 cm i.d mold. 65

Figure 4.17:	Comparison of magnitude of thermal build-up in between treated and non-treated monoliths. Polymerizations were carried out at a constant monomer ratio (EDMA/GMA) of 30/70; porogen concentration of 70 %; polymerization temperature of 60 °C; monolith dimension: 5.0 cm i.d, 150 ml; AIBN concentration of 1 % (w/w) of monomers.	67
Figure 4.18:	Comparison of pore size distribution patterns in between a) pre-modified and b) post-modified monoliths. Polymerizations were carried out at a constant monomer ratio (EDMA/GMA) of 30/70; porogen concentration of 70 %; polymerization temperature of 60 °C; monolith dimension: 5.0 cm i.d, 150 ml; AIBN concentration of 1 % (w/w) of monomers.	69
Figure 4.19:	Comparison of surface morphology in between pre-modified and post-modified monoliths. Polymerizations were carried out at a constant monomer ratio (EDMA/GMA) of 30/70; porogen concentration of 70 %; polymerization temperature of 60 °C; monolith dimension: 5.0 cm i.d, 150 ml; AIBN concentration of 1 % (w/w) of monomers.	70
Figure 4.20:	3D diagram of pump-driven monolith reactor from a) top, b) front, c) left and d) right view.	73
Figure 4.21:	Red zone of MR-03 features thermostated waterbath and thermal insulated reservoir with both having circulated pipe configuration driven by submerged aquarium water pumps.	75
Figure 4.22:	Blue zone of MR-03 features chiller bath and thermal insulated reservoir with both having circulated pipe configuration driven by submerged aquarium water pumps.	76
Figure 4.23:	Violet zone of MR-03 features a 50 L reactor tank connected to an external gear hydro pump. The piping is	76

configured to receive and return back the water from and to both red zone and blue zone.

Figure 4.24:	Complete representation of piping setup.	78
Figure 4.25:	VBA (Visual Basic for Application) coding for Microsoft Excel that enabled logging of temperature data at per minute interval.	80
Figure 4.26:	Interface of the controller based on Microsoft Excel.	81
Figure 4.27:	Comparison of 3 different modes of controller configuration. Polymerizations were carried out at a constant monomer ratio (EDMA/GMA) of 30/70; porogen concentrations of 60 %; polymerization temperature of 50 °C; monolith dimension: 17.0 cm i.d, diameter : height ratio of 1 : 1; AIBN concentration of 1 % (w/w) of monomers.	83
Figure 4.28:	Maximum temperature recorded for each controller configuration. 0 = negative control; 1 = 1 <sup>st</sup> mode; 2 = 2 <sup>nd</sup> mode; 3 = 3 <sup>rd</sup> mode. Polymerizations were carried out at a constant monomer ratio (EDMA/GMA) of 30/70; porogen concentrations of 60 %; polymerization temperature of 50 °C; monolith dimension: 17.0 cm i.d, diameter : height ratio of 1 : 1; AIBN concentration of 1 % (w/w) of monomers.	83
Figure 4.29:	Time span prior to the emergence of thermal build-up.	84
Figure 4.30:	Thermographic analysis of the monolith fabrication process at progressive timeline.	86

## LIST OF ABBREVIATIONS

<b>DNA</b>	- Deoxyribonucleic acid
<b>ROI</b>	- Return of investment
<b>PEG</b>	- Polyethylene glycol
<b>HPLC</b>	- High performance liquid chromatography
<b>BSA</b>	- Bovine serum albumin
<b>IEX</b>	- Ion Exchange
<b>IgG</b>	- Immunoglobulin G
<b>NAD<sup>+</sup></b>	- Nicotinamide adenine dinucleotide
<b>TMOS</b>	- Tetramethoxysilane
<b>PEO</b>	- Polyethylene oxide
<b>PEEK</b>	- Polyether ether ketone
<b>HSA</b>	- Human serum albumin
<b>GMA</b>	- Glycidyl methacrylate
<b>EDMA</b>	- Ethylene dimethacrylate
<b>µm</b>	- Micrometer
<b>CIM</b>	- Convective interaction media
<b>AIBN</b>	- Azobisisobutyronitrile
<b>CDI</b>	- Carbonyldiimidazole
<b>DSC</b>	- Disuccinimidyl carbonate
<b>cm</b>	- Centimeter
<b>mm</b>	- Milimeter
<b>Na<sub>2</sub>CO<sub>3</sub></b>	- Sodium carbonate
<b>CO<sub>2</sub></b>	- Carbon dioxide
<b>SC-CO<sub>2</sub></b>	- Supercritical carbon dioxide
<b>PSI</b>	- Per square inch
<b>TMPTMA</b>	- Trimethylolpropane-trimethacrylate
<b>BMA</b>	- Butyl methacrylate
<b>EGDMA</b>	- Ethylene glycol dimethacrylate
<b>i.d</b>	- Internal diameter
<b>mL</b>	- Milliliter

<b>nm</b>	-	Nanometer
<b>ROMP</b>	-	Ring-opening metathesis polymerization
<b>NBE</b>	-	Norborn-2-ene
<b>RuCl<sub>2</sub>(PCy<sub>3</sub>)<sub>2</sub>(CHP)</b>	-	First-generation Grubbs initiator
<b>h)</b>	-	
<b>UV</b>	-	Ultraviolet
<b>RTILs</b>	-	Room temperature ionic liquids
<b>kGy</b>	-	Kilogray
<b>PAN</b>	-	Polyacrylonitrile
<b>DMSO</b>	-	Dimethyl sulfoxide
<b>TIPS</b>	-	Thermally induced phase separation
<b>°C</b>	-	Degree celcius
<b>m<sup>2</sup></b>	-	Square meter
<b>g</b>	-	Gram
<b>TEOS</b>	-	Tetraethyl orthosilicate
<b>TBOF</b>	-	Tetrabutyl ammonium fluorid
<b>m<sup>2</sup>g<sup>-1</sup></b>	-	Square meter per gram
<b>cm<sup>3</sup>g<sup>-1</sup></b>	-	Cubic centimeter per gram
<b>Wt%</b>	-	Percentage by weight
<b>Hr</b>	-	Hour
<b>PFA</b>	-	Polyfurfuryl alcohol
<b>mL g<sup>-1</sup></b>	-	Mililiter per gram
<b>PEGDA</b>	-	Polyethylene (glycol) diacrylate
<b>PPO</b>	-	Poly(propylene)glycols
<b>NaOH</b>	-	Sodium hydroxide
<b>HIEPE</b>	-	High internal phase emulsion
<b>φ</b>	-	High internal phase volume ratio
<b>SEM</b>	-	Scanning electron microscope
<b>PVA</b>	-	Polyvinyl alcohol
<b>CTAB</b>	-	Hexadecyltrimethylammonium bromide
<b>SDS</b>	-	Sodium dodecyl sulfate

<b>RAFT</b>	- Reversible addition-fragmentation chain transfer
<b>kbp</b>	- Kilobase pairs
<b>T<sub>poly</sub></b>	- Polymerization temperature
<b>T<sub>max</sub></b>	- Maximal temperature
<b>pH</b>	- Potential Hydrogen
<b>FRP</b>	- Free radical polymerization
<b>R<sup>2</sup></b>	- Coefficient of determination
<b>T<sub>sp</sub></b>	- Temperature setpoint for chiller/waterbath
<b>NGC</b>	- Next generation chromatography
<b>VBA</b>	- Visual basic for application
<b>L</b>	- Liter
<b>w/w</b>	-
<b>ΔT<sub>max</sub></b>	- Differential maximum temperature value recorded in between two monoliths Differential maximum temperature value recorded at core region in between two monoliths
<b>T<sub>waterbath</sub></b>	- Temperature of waterbath
<b>≈</b>	- Approximate
<b>&lt;</b>	- Less than
<b>T<sub>chiller</sub></b>	- Temperature of chiller
<b>CAD</b>	- Computer aided design
<b>T<sub>forecast</sub></b>	- Predicted temperature
<b>T<sub>present</sub></b>	- Present/Current/Live temperature value
<b>T<sub>previous</sub></b>	- Previous temperature value
<b>T<sub>surface</sub></b>	- Temperature measured at surface of monolith
<b>V<sub>pore</sub></b>	- Volume of pore fraction
<b>W<sub>wet</sub></b>	- Weight of wet adsorbent fragment
<b>W<sub>Dry</sub></b>	- Weight of dry adsorbent fragment

<b>g/cm<sup>3</sup></b>	- Density
<b>V<sub>Mold</sub></b>	- Volume of clay mold
<b>V<sub>Adsorbent</sub></b>	- Volume of adsorbent fragment
<b>SOP</b>	- Standard operating procedure



**UMS**  
UNIVERSITI MALAYSIA SABAH